THE EFFECTS OF CHOLESTEROL ON LATERAL DIFFUSION AND VERTICAL FLUCTUATIONS IN LIPID BILAYERS

An Electron-Electron Double Resonance (ELDOR) Study

JUN-JIE YIN, JIM B. FEIX, AND JAMES S. HYDE
National Biomedical ESR Center, Department of Radiology, Medical College of Wisconsin, Milwaukee, Wisconsin 53226

ABSTRACT Electron-electron double resonance (ELDOR) and saturation-recovery spectroscopy employing ^{14}N:^{15}N stearic acid spin-label pairs have been used to study the effects of cholesterol on lateral diffusion and vertical fluctuations in lipid bilayers. The ^{14}N:^{15}N continuous wave electron-electron double resonance (CW ELDOR) theory has been developed using rate equations based on the relaxation model. The collision frequency between ^{14}N-16 doxyl stearate and ^{15}N-16 doxyl stearate, W_{Hex} (16:16), is indicative of lateral diffusion of the spin probes, while the collision frequency between ^{14}N-16 doxyl stearate and ^{15}N-5 doxyl stearate, W_{Hex} (16:5), provides information on vertical fluctuations of the ^{14}N-16 doxyl stearate spin probe toward the membrane surface. Our results show that: (*a*) cholesterol decreases the electron spin-lattice relaxation time T_{1e} of ^{14}N-16 doxyl stearate spin label in dimyristoylphosphatidylcholine (DMPC) and egg yolk phosphatidylcholine (egg PC). (*b*) Cholesterol increases the biomolecular collision frequency W_{Hex} (16:16) and decreases W_{Hex} (16:5), suggesting that incorporation of cholesterol significantly orders the part of the bilayer that it occupies and disorders the interior region of the bilayer. (*c*) Alkyl chain unsaturation of the host lipid moderates the effect of cholesterol on both vertical fluctuations and lateral diffusion of ^{14}N-16 doxyl stearate. And (*d*), there are marked differences in the effects of cholesterol on lateral diffusion and vertical fluctuations between 0–30 mol% and 30–50 mol% of cholesterol that suggest an inhomogeneous distribution of cholesterol in the membrane.

INTRODUCTION

Cholesterol and phospholipids are two major components of cell membranes, and their interaction has been the subject of extensive studies. The exact role of cholesterol in membrane structure and function has remained elusive, as indicated by many controversies concerning the stoichiometry of lipid-cholesterol complex formation (1).

Various techniques have been used to study the effect of cholesterol on the motional properties of lipids in membranes, including electron spin resonance (ESR) spectroscopy. In conventional ESR spin-label studies, the rotational diffusion constant (2), the order parameter, S (3–5), and the maximum line splitting, T (3, 6, 7) have been used to describe rotational motions of lipid-analogue spin labels in the hydrophobic region of the bilayer as a function of cholesterol concentration. These methods are particularly sensitive to rotational motions of the spin probes. There is a general agreement that increasing cholesterol produces a gradual inhibition of rotational mobility for spin labels in fluid-phase bilayers (3–6). This reduction in fluidity is also observed by fluorescence (8, 9) and deuterium nuclear magnetic resonance (NMR) (5) studies that focus on the rotational motion.

Lipid lateral diffusion in membranes (i.e., two-dimensional translational diffusion parallel to the plane of the bilayer) is believed to be an important physical characteristic of biological membranes. However, in contrast to studies of rotational diffusion, in only a few works has the effect of cholesterol on lateral diffusion of lipids in model membranes been investigated. The results remain somewhat controversial. In the fluid phase, cholesterol appears to decrease the lateral diffusion constant of membrane lipids as studied by fluorescence photobleaching techniques (10–12). Kuo and Wade (13), using a pulse NMR method, found that cholesterol in small amounts (<10 mol%) produces a large increase in lipid lateral diffusion followed by a gradual decrease in lipid diffusion rates as the level of cholesterol is increased. Lindblom et al. (14), also using pulse-gradient NMR, found a slight increase in lipid diffusion over the range of 0 to 30 mol% cholesterol. Thus photobleaching recovery and pulse-

Please address all correspondence to Dr. James S. Hyde.

gradient NMR have provided distinctly different results for the effect of cholesterol on lipid lateral diffusion.

During the past several years, the continuous wave electron-electron double resonance (CW ELDOR) method has been employed to measure lateral diffusion of lipids in model membranes (15, 16) and intact cell membranes (17, 18). ELDOR, in conjunction with saturation recovery, can determine the spin-exchange rate, which is a direct reflection of bimolecular collisions between spin probes. ELDOR methods provide determination of exchange frequencies with a much lower spin-label concentration than is possible by observing the effects of spin exchange on linewidth (19).

The method depends upon Heisenberg exchange between nitroxide-radical spin labels. Bimolecular collisions between spin labels given rise to Heisenberg exchange that results in transfer of saturation between hyperfine lines of the spin label. There is another competing saturation-transfer mechanism, nitrogen nuclear spin-lattice relaxation of the spin label, characterized by (W_n). Recently, Feix et al. (16) introduced ^{14}N:^{15}N spin-label pairs in an ELDOR study. This technique eliminates the problem of intramolecular contributions to the ELDOR effect from the nitrogen nuclear relaxation. When using ^{14}N:^{15}N stearic acid spin-label pairs with the two isotopes at the same depth, they could obtain lateral diffusion data. With the ^{14}N and ^{15}N nitroxide moieties at different positions, "vertical fluctuations" of the acyl chain could be measured.

We develop here the theory of ^{14}N:^{15}N CW ELDOR by analyzing rate equations based on a relaxation model that includes the Heisenberg exchange rate, W_{Hex}, the electron spin-lattice relaxation rate, W_e, and the concentrations of the spin probes.

The major purpose of the present work was to use the ^{14}N:^{15}N CW ELDOR technique to investigate the effects of cholesterol on lateral diffusion and vertical fluctuations of lipids. Different mole percentages of cholesterol in dimyristoylphosphatidylcholine (DMPC) were used to survey translational motion of stearic acid spin labels in fluid regions I and III in the phase diagram (20) of DMPC. Egg yolk phosphatidylcholine (egg PC) was used to study the effect of the alkyl chain unsaturation on lipid-cholesterol interaction.

THEORY

ELDOR has been reviewed by Kevan and Kispert (21). Two powers must be incident on the sample: a pumping field that is sufficient to cause saturation, and an observing field that is generally much lower.

Saturation transfer through different relaxation pathways can be studied by either time domain-ESR or by CW ELDOR. In CW ELDOR the pump field exists throughout the experiment.

If the hyperfine lines are strongly coupled by nitrogen nuclear relaxation and two isotopes are employed, the appropriate energy-level diagram is that shown in Fig. 1, where W_s is the transition probability associated with the pumping microwave source, W_{e1}, W_{e2} are the electron spin-lattice relaxation rates for the two species, and K_x is the spin-exchange rate constant in units of $\ell(\text{mol} \cdot \text{s})^{-1}$.

Spin system I is pumped and system II is observed. If the observing power is sufficiently low, the rate equations are the following:

$$\frac{d(n_1 - n_2)}{dt} = -2W_{e1}[(n_1 - n_2) - (N_1 - N_2)] + 2K_x(n_2n_3 - n_1n_4) - 2W_s(n_1 - n_2), \quad (1)$$

$$\frac{d(n_3 - n_4)}{dt} = -2W_{e2}[(n_3 - n_4) - (N_3 - N_4)] - 2K_x(n_2n_3 - n_1n_4), \quad (2)$$

where lower case n's are the instantaneous populations per unit volume of the four levels and upper cases N's are the equilibrium Boltzmann populations per unit volume. Since

$$n_2n_3 - n_1n_4 = (1/2)[N_{II}(n_2 - n_1) + N_I(n_3 - n_4)], \quad (3)$$

and trivially,

$$2W_s(n_1 - n_2) = 2W_s[(n_1 - n_2) - (N_1 - N_2)] + 2W_s(N_1 - N_2), \quad (4)$$

where N_I and N_{II} are the concentrations of spin system I and II, respectively, ($n_1 + n_2 = N_I$; $n_3 + n_4 = N_{II}$), Eqs. 1 and 2 can be shown to be linear differential equations.

Let:

$$i_I = (n_1 - n_2) - (N_1 - N_2); \qquad i_{II} = (n_3 - n_4) - (N_3 - N_4). \quad (5)$$

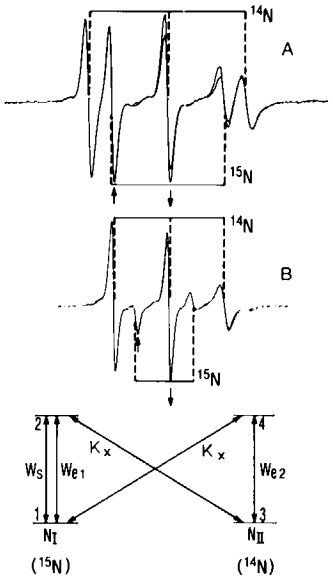

FIGURE 1. ELDOR effect for (*A*) the ^{14}NC16:^{15}NC16 (0.5 : 0.25 mol%) and (*B*) ^{14}NC16:^{15}NC5 (0.5 : 0.5 mol%) stearic acid spin labels in DMPC at 37°C, pH 9.5. Superimposed spectra were recorded with the pump field off and on at 400 mW. Arrows define the position of the pumping field (↑) when the observe field (↓) is on the center line of ^{14}N ($M_I = 0$). (*C*) The relaxation model. Because of very fast nuclear relaxation, hyperfine lines of each isotope are assumed to be strongly coupled.

After some rearrangement, Eqs. 1 and 2 become

$$\frac{di_I}{dt} = -(2W_{e1} + N_{II}K_x + 2W_s)i_I + N_I K_x i_{II} - 2W_s(N_I - N_2), \quad (6)$$

$$\frac{di_{II}}{dt} = -(2W_{e2} + N_I K_x)i_{II} + N_{II} K_x i_I. \quad (7)$$

Since the CW ELDOR experiment is under steady state conditions,

$$\frac{di_I}{dt} = \frac{di_{II}}{dt} = 0, \quad (8)$$

and Eqs. 5 and 6 become:

$$i_I = \frac{-W_s(N_I - N_2)(2W_{e2} + N_I K_x)}{2W_{e1}W_{e2} + W_{e1}N_I K_x + W_{e2}N_{II}K_x + W_s(2W_{e2} + N_I K_x)}, \quad (9)$$

$$i_{II} = \frac{-W_s(N_I - N_2)N_{II}K_x}{2W_{e1}W_{e2} + W_{e1}N_I K_x + W_{e2}N_{II}K_x + W_s(2W_{e2} + N_I K_x)}. \quad (10)$$

Let the ESR signal be proportional to the instantaneous population difference, with a constant of proportionality C:

$$i = C(n_3 - n_4).$$

Without pumping (i.e., $W_s = 0$)

$$i_{IIoff} = C(n_3 - n_4) = C(N_3 - N_4). \quad (11)$$

With the pumping field on,

$$i_{IIon} = C[(N_3 - N_4) + i_{II}]. \quad (12)$$

From the definition of ELDOR reduction (22)

$$R = 1 - \frac{i_{IIon}}{i_{IIoff}} = \frac{-i_{II}}{(N_3 - N_4)}. \quad (13)$$

So, we have

$$R^{-1} = \frac{2W_{e1}W_{e2} + W_{e1}N_I K_x + W_{e2}N_{II}K_x}{W_s \times N_I K_x} + \frac{2W_{e2} + N_I K_x}{N_I K_x}. \quad (14)$$

Eq. 14 predicts that a plot of R^{-1} versus W_s^{-1} (i.e., the inverse of the pump power) will be linear with an intercept that depends on the Heisenberg exchange rate constant.

As the pumping power goes to infinity ($W_s \rightarrow \infty$)

$$R_\infty^{-1} = \frac{(2W_{e2} + N_I K_x)}{N_I K_x}. \quad (15)$$

The Heisenberg exchange frequency W_{Hex} becomes:

$$W_{Hex} = N_I K_x = 2(R_\infty^{-1} - 1)^{-1} W_{e2}. \quad (16)$$

Eq. 16 shows that experimental knowledge of the intercept at infinite power, R_∞^{-1}, the concentration of pumped species, and the spin-lattice relaxation rate of the observed species permits determination of the Heisenberg exchange rate constant. A rate constant must, of course, be independent of the concentrations of reacting species, N_I and N_{II}. This prediction can easily be tested experimentally.

MATERIALS AND METHODS

The ^{15}N stearic acid spin label 2-(14-carboxytetradecyl)-1-ethyl-4,4-dimethyl-3-oxyzlidinoxyl (designated here as $^{15}NC16$) and 2-(3-carboxypropyl)-4,4-dimethyl-2-tridecyl-3-oxazolidinoxyl (designated here as $^{15}NC5$) were synthesized according to the method of Venkataramu et al. (23) and were a gift from Prof. J. H. Park. $^{14}NC16$ was from Aldrich Chemical Co., Milwaukee, WI.

Dimyristoylphosphatidylcholine (DMPC) was from Sigma Chemical Co., St. Louis, MO. Egg yolk phosphatidylcholine (>99% pure) was from Avanti Polar Lipids, Inc., Birmingham, AL, and cholesterol (crystallized) from Boehringer-Mannheim Diagnostics, Inc., Indianapolis, IN.

Stock solutions of the spin labels and lipids were prepared in chloroform and stored at −20°C. The buffer was 0.1 M borate at pH 9.5 to insure that all stearic acid carboxyl groups in the phosphatidylcholine membranes were ionized (6, 16). Multilamellar liposomes were prepared by directly hydrating the dried lipids and spin labels with an appropriate amount of buffer as described previously (16). All samples were run in capillaries made of the methylpentene polymer TPX (0.6 mm i.d.). A flow of temperature-regulated nitrogen gas over the capillary was used to remove oxygen (24).

A loop-gap resonator was used for the ELDOR experiments (17). Both pumping and observing microwave frequencies were fed to the resonator. The Q of resonator is quite low, of the order of 300, corresponding at X band to 30 MHz between 3 dB points. This low Q is compensated by the high energy density for a given input power resulting in a high ηQ product, where η is the filling factor. All measurements were made with the pumping frequency on resonator resonance and the observing frequency off resonance. This provides the best isolation of pumping and observing microwave fields. ELDOR experiments were performed as described in our previous studies (16, 17). ELDOR reductions were measured from the center line of ^{14}N when the low field line of ^{15}N was pumped (Fig. 1). The low field line of ^{14}N was used for normalization.

ELDOR reduction factors were determined at a series of nine pumping intensities and R^{-1} plotted against the inverse of pumping power P^{-1} (25). Extrapolation to infinite pumping power gives the intercept R_∞^{-1}, which is a function of the relaxation processes occurring in the spin system as shown in Eq. 15. The W_{Hex} values were calculated from the experimental data via Eq. 16. The Heisenberg exchange frequency W_{Hex} represents the bimolecular collision frequncy of an ^{14}N spin label with ^{15}N probes.

In order to obtain the absolute value of the Heisenberg exchange rate, W_{Hex}, one must determine the spin-lattice relaxation time T_{1e}. T_{1e} can be estimated by CW saturation techniques, but the time-domain method of saturation recovery is preferable. The saturation-recovery spectrometer is based on the design of Huisjen and Hyde (26). A multichannel signal acquisition system greatly improves the signal-to-noise ratio over what could be achieved with the single channel boxcar. A FET microwave amplifier has been introduced. A low-pass filter of high order before the A/D converter cuts off at 25 MHz, which results in minimal distortion of the transient signal. In the present work, the saturation-recovery time constants are those of the transition observed (i.e., the ^{14}N center line) in the corresponding ELDOR experiments (Eqs. 15 and 16) and all T_{1e} values were measured on that line in the same system before addition of ^{15}N spin probe. Typically, 2×10^4 decays per second were acquired with 512 data points on each decay. The accumulation time was 5 min. Aperture intervals were 20 or 30 ns.

In the long-duration-pulse saturation-recovery experiment, the tail of the decay curve approximates a single exponential (27). The T_{1e} values

were from the tail of the recovery curve and were independent of pulse length (>5 μs) and observe power (H_1 < 0.1 G).

Conventional ESR spectra were obtained on an ESR spectrometer (Varian Associates, Palo Alto, CA) in normal configuration. Spectra were obtained with 5 mW incident microwave power and 100 kHz field modulation of 0.5 G. The order parameters S were calculated using the conventional method (28).

RESULTS

Field-swept CW ELDOR spectra of ^{14}NC16:^{15}NC16 (16:16) and ^{14}NC16:^{15}NC5 (16:5) spin-label pairs in DMPC at 37°C are shown in Fig. 1. The frequency difference between pumping and observing microwave sources was 26 and 24 MHz for the ^{14}NC16:^{15}NC16 and ^{14}NC16:^{15}NC5 ELDOR experiments, respectively.

Fig. 2 shows experimental results with different concentrations of ^{14}NC16 and ^{15}NC16 spin label pairs in DMPC. There is a linear dependence of R^{-1} on the reciprocal pumping power $(P)^{-1}$, as predicted by Eq. 14. The slope depends on the concentrations of both pumped and observed spin species. The intercept, R_∞^{-1}, depends only on the concentration of the pumped spin species, as does the Heisenberg exchange frequency, W_{Hex}, as predicted by Eq. 16.

The effective Heisenberg exchange rate constants (which we define as [Heisenberg exchange frequency/concentration ratio label/lipid]) for 0.1 and 0.33 mol% concentration of the pumped species are, using Eq. 16, 0.88×10^8 and 0.87×10^8. A consistent analysis requires that these values be independent of the concentration of the pumped species, as observed.

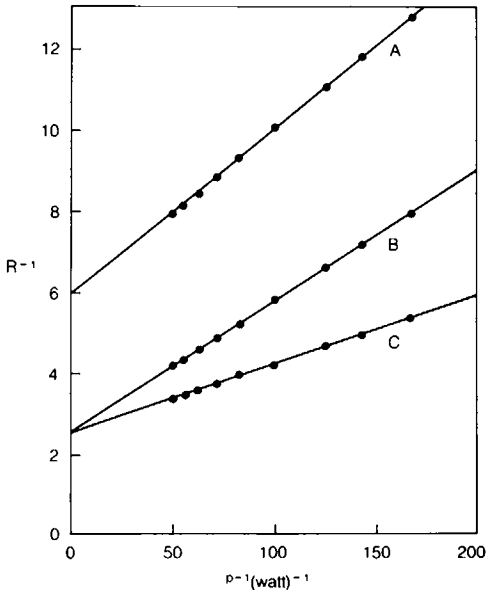

FIGURE 2. Experimental test of model in DPMC at 37°C, pH 9.5, demonstrating that the ELDOR reduction is linear in the inverse of pumping power, p^{-1}. The concentrations of spin-label pairs ^{14}NC16 (observed) : ^{15}NC16(pumped) were (A) 0.1 : 0.1 mol%; (B) 0.25 : 0.33 mol%; and (C) 0.1 : 0.33 mol%. The slopes are (A) 0.815; (B) 0.657; and (C) 0.343. The intercepts R_∞^{-1} are (A) 5.98; (B) 2.53; and (C) 2.52.

As shown in Figs. 3, 4, and Table I, the effective T_{1e} of ^{14}NC16 spin label in DMPC is shortened by incorporation of cholesterol. T_{1e} of ^{14}NC16 decreases in egg PC continuously with increasing cholesterol. A similar tendency was found in DMPC with a broad maximum at 30 mol% cholesterol.

The faster relaxation of ^{14}NC16 suggests that incorporation of cholesterol increases the rate of rotational motion for the nitroxide moiety near the center of the bilayer (15). This has also been noted for certain fluorescent probes (9).

ELDOR reduction factors (R_∞) for the ^{14}NC16:^{15}NC16 and ^{14}NC16:^{15}NC5 spin-label pairs in DMPC and egg PC with different cholesterol concentrations are given in Table II, and shown in Figs. 5 and 6. The ELDOR reduction for ^{14}NC16:^{15}NC16 in DMPC and egg PC increases with increasing cholesterol to a maximum at 30 mol% cholesterol. This is despite a shortening of T_{1e} (Table I), which limits the time available for interaction between the spin labels. Above 30 mol% cholesterol, R_∞ values for the 16:16 pair diminish somewhat, with effects in DMPC and egg PC being similar.

For the ^{14}NC16:^{15}NC5 spin-label pair, ELDOR reduc-

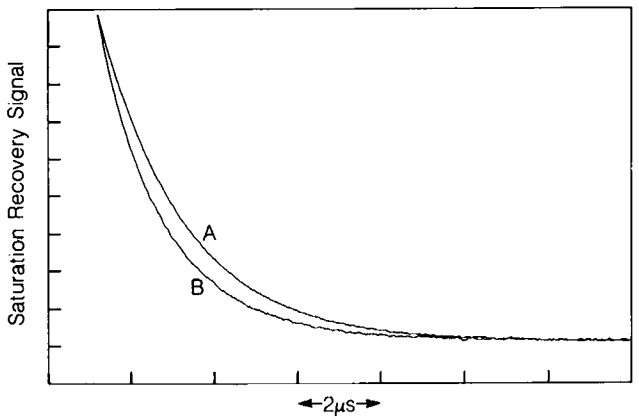

FIGURE 3. Saturation-recovery signal of ^{14}NC16 (0.5 mol%) in DMPC liposomes at 37°C, pH 9.5 (A) no cholesterol; (B) with 30 mol% cholesterol. Each recovery signal obtained in 5 min at 20,000 accumulations per second, 512 data points accumulation.

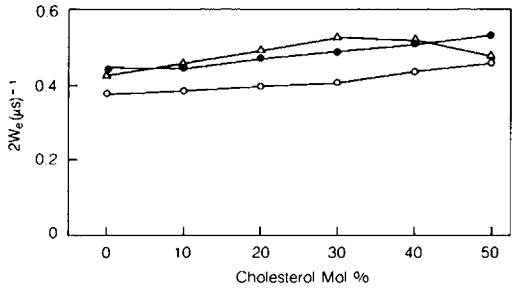

FIGURE 4. Inverse of the spin-lattice relaxation time $(T_{1e})^{-1}$ of ^{14}NC16 as a function of mole fraction of cholesterol in (△) DMPC at 37°C; (●) egg PC at 37°C; (○) egg PC at 27°C. Data are for 37°C as given in Table I.

TABLE I
SPIN-LATTICE RELAXATION TIMES
FOR ^{14}N 16-DOXYL STEARATE

Cholesterol	Egg PC	DMPC
mol%	$\times 10^6$ *s*	$\times 10^6$ *s*
0	2.24	2.29
10	2.20	2.20
20	2.11	2.01
30	2.05	1.90
40	1.96	1.96
50	1.89	2.09

^{14}N-16 Doxyl stearate was present at 0.5 mol%. Membranes were equilibrated with 0.1 M borate, pH 9.5 (see text). Data are for 37°C.

TABLE II
ELDOR REDUCTIONS FOR THE 16:16 AND 16:5
SPIN-LABEL PAIRS

Cholesterol	Egg PC		DMPC	
	R_∞ (16:16)%	R_∞ (16:5)%	R_∞ (16:16)%	R_∞ (16:5)%
mol%				
0	29.9	23.7	31.6	31.3
10	31.4	23.1	32.7	28.6
20	35.2	21.7	35.8	24.3
30	36.7	18.5	38.3	17.5
40	34.5	16.6	33.6	14.5
50	33.7	15.6	32.9	13.3

R_∞ values are the inverse of R_∞^{-1}, determined experimentally (as in Fig. 2). Samples contained 0.5 mol% ^{14}N-16 doxyl stearate and either 0.5 mol% ^{15}N-5 doxyl stearate or 0.25 mol% ^{15}N-16 doxyl stearate and were equilibrated with 0.1 M borate, pH 9.5, as described in the text. Data are for 37°C.

tions progressively decrease with increasing cholesterol content. There is a significant difference between DMPC and egg PC, with the effect of cholesterol on vertical fluctuations in DMPC stronger than in egg PC. The most pronounced effects occur from 0 to 30 mol% in DMPC.

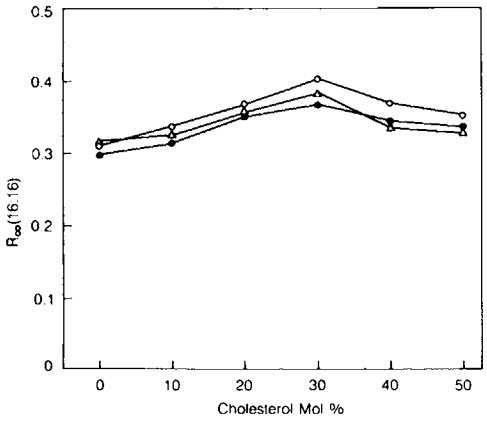

FIGURE 5. ELDOR reduction R_∞ of ^{14}NC16:^{15}NC16 (0.5 : 0.25 mol%) as a function of mole fraction of cholesterol in (△) DMPC at 37°C; (●) egg PC at 37°C; (○) egg PC at 27°C. Data are for 37°C as given in Table II.

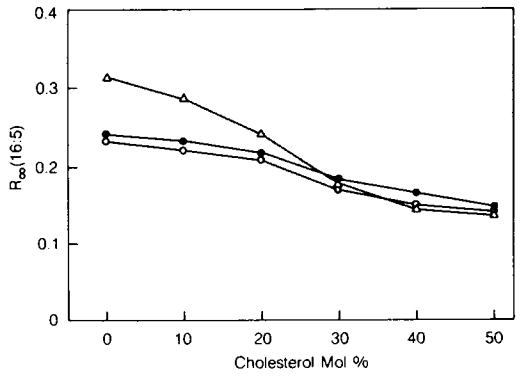

FIGURE 6. ELDOR reduction R_∞ of ^{14}NC16:^{15}NC5 (0.5 : 0.5 mol%) as a function of mole fraction of cholesterol in (△) DMPC at 37°C; (●) egg PC at 37°C; (○) egg PC at 27°C.

Fig. 7 shows the effects of cholesterol on the bimolecular collision rate W_{Hex} (16:16) in DMPC and egg PC. W_{Hex} for 16:16 in DMPC shows a sharp increase from 0 to 30 mol% cholesterol, beyond which (i.e., from 30 to 50% cholesterol) the 16:16 interaction frequency decreases. In egg PC the 16:16 interaction also increases between 0 and 30 mol% cholesterol, though more gradually than in DMPC. W_{Hex} for 16:16 in egg PC levels off above 30 mol% cholesterol, with only a slight decrease at higher cholesterol content.

The measured exchange rates W_{Hex} (16:5) as a function of cholesterol mole fraction for egg PC and DMPC are shown in Fig. 8. The vertical fluctuations of ^{14}NC16 decrease monotonically as the mole fraction of cholesterol increases in both DMPC and egg PC. Again, the effects of cholesterol are more pronounced in DMPC than in egg PC.

The effect of cholesterol on vertical fluctuations of ^{14}NC16 in DMPC and egg PC also is shown by the ratio of W_{Hex} (16:5)/W_{Hex} (16:16), normalized to the same probe concentration (Fig. 9). As discussed previously (29), expressing the data in this fashion takes into account the fact that the molecules carrying nitroxide probes must come together before they can interact, regardless of the

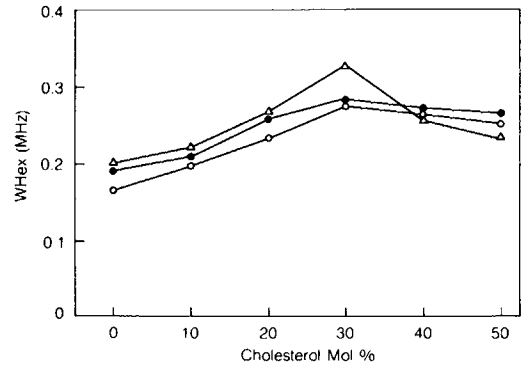

FIGURE 7. Heisenberg exchange rates for the ^{14}NC16:^{15}NC16 (0.5 : 0.25 mol%) spin-label pairs in (△) DMPC at 37°C; (●) egg PC at 37°C; (○) egg PC at 27°C.

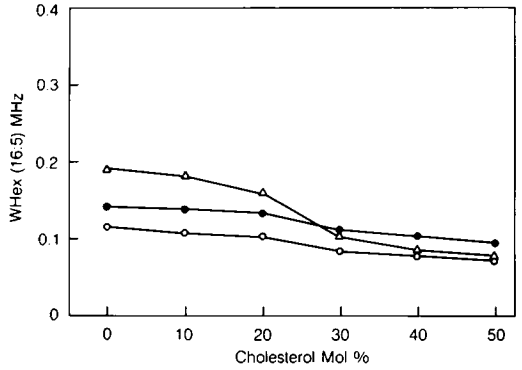

FIGURE 8. Heisenberg exchange rates for the ^{14}NC16:^{15}NC5 (0.5 : 0.5 mol%) spin-label pairs in (△) DMPC at 37°C; (●) egg PC at 37°C; (○) egg PC at 27°C.

position of the nitroxide moiety on the carrier molecule (in this case along the stearic acid alkyl chain). This serves to emphasize the vertical fluctuation component of the 16:5 interaction in situations where lateral diffusion might also be influenced. Fig. 9 demonstrates with this treatment of the data strong effects of cholesterol on vertical fluctuations. From 0 to 30 mol%, cholesterol produces a profound inhibition of the normalized 16:5 interaction frequency. The relative probability of 16:5 interaction with the incorporation of 30 mol% cholesterol (relative to no cholesterol) is diminished by 63% in DMPC and by 48% in egg PC (both at 37°C). As seen in Fig. 9, the effects of cholesterol on vertical fluctuations appear to plateau in the region of 30 mol%, with no further diminution at higher cholesterol content. As in the other studies presented here, the effects of cholesterol are greater in DMPC than in egg PC.

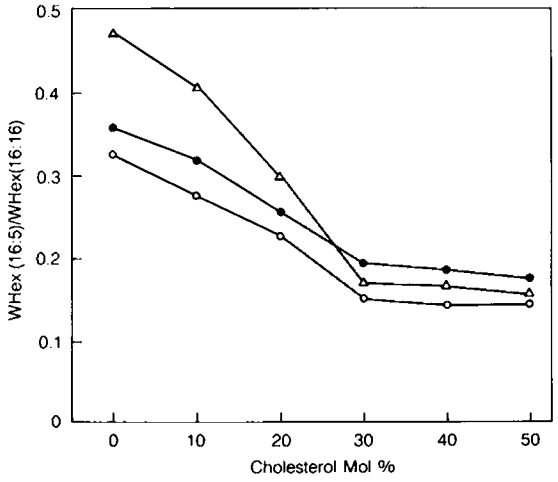

FIGURE 9. Reduction probability of vertical fluctuation as a function of mole fraction of cholesterol. Shown are the Heisenberg exchange rates for ^{14}NC16:^{15}NC5 pairs normalized to the ^{14}NC16:^{15}NC16 exchange frequency for (△) DMPC at 37°C; (●) egg PC at 37°C; (○) egg PC at 27°C. The mole fraction of the pumped species was 0.5% for both spin-label pairs.

DISCUSSION

In principle, saturation transfer through various relaxation processes could be studied by both CW ELDOR and time-domain ESR methods. In CW ELDOR, the reduction is the general result of a multiplicity of superimposed relaxation processes, whereas in time-domain ESR the dynamic processes result in superimposed multiexponential signals that at least in principle can be deconvoluted. However, CW ESR method generally result in better signal-to-noise ratio than pulse methods. We plan to study these same systems further using the short-pulse saturation-recovery technique (27), which may give more detailed information.

In this work we have used the rate equation method to develop ELDOR theory in a thorough and general manner. The rate equation method has been used previously in a simpler problem by Yoshida et al. (30), and is based on approaches developed a number of years ago for analysis of cross relaxation ESR experiments in solids (see Stanley and Vaughn [29]). The results obtained with this approach are identical to those obtained using the theory developed by Freed (31). The theoretical development presented here predicts that in a dual-label system the ELDOR reduction extrapolated to infinite pump power is dependent only on the concentration of the pumped species, T_{1e} of the observed species, and the bimolecular collision rate (Eq. 16). This is in agreement with experimental results (Fig. 2).

The order parameter S for ^{14}NC16 is shown in Fig. 10. Thus we have four comparable displays indicative of motion in the lipid bilayer: Fig. 4 showing the spin-lattice relaxation rate; Fig. 7 showing lateral diffusion; Fig. 9 showing vertical fluctuations; and Fig. 10 showing rotational motions. Probably spin-lattice relaxation data at a single microwave frequency are not very informative, but the other displays are useful. W_{Hex} (16:16) and W_{Hex} (16:5) provide dynamic information on the bimolecular collision rates between spin labels on a time scale of W_{e2}, while the order parameter reports on a time-independent distribu-

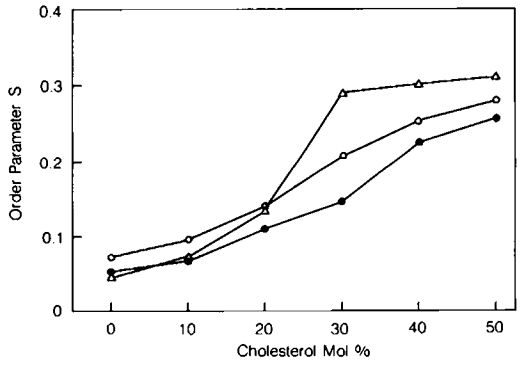

FIGURE 10. Order parameter S of ^{14}NC16 as a function of mole fraction of cholesterol in (△) DMPC at 37°C; (●) egg PC at 37°C; (○) egg PC at 27°C.

tion of spin-label motion and orientation. The W_{Hex} (16:5) display is sensitive to the rotational mobility of the spin labels. The order parameter and vertical fluctuation data are broadly consistent in indicating that cholesterol impedes rotational motion near the surface of the bilayer. But the order parameter display shows greater differences at high cholesterol concentration and the vertical fluctuation data show greater differences at low concentrations. The increase in W_{Hex} (16:16) from 0 to 30 mol% cholesterol (Fig. 7) that occurs under conditions where rotational motions (Figs. 9 and 10) decrease is striking indeed. Cholesterol has a dual effect: both fluidizing and ordering, depending on the aspect of motion being considered.

All four key displays of data in this paper (Figs. 4, 7, 9, 10) show breaks at 30 mol% for DMPC. It is notable that at 37°C in DMPC the 0–30 mol% and 30–50 mol% cholesterol regions correspond to regions I and III in the phase diagram (20) of Recktenwald and McConnell. Both translational and rotational motion displays are sensitive to the phase boundary.

Presti and Chan (7) proposed that as cholesterol is added to phospholipid bilayers, two phases exist in the mixture, a free lipid phase and a lipid-cholesterol phase. Above a composition of 30 mol% cholesterol, only the cholesterol-rich domain remains. We note that there could be different collision frequencies in the different environments. Indeed, the observed increase in W_{Hex} (16:16) with the addition of cholesterol up to 30 mol% may arise from preferential partitioning of the stearic acic spin labels into more fluid, cholesterol-free domains. This would increase the effective mole fraction of spin label in restricted regions of the bilayer, with a concomitant increase in the bimolecular collision frequency. Further experiments using spin labels with more reliable partitioning behavior (i.e., phospholipid spin labels) may permit more conclusive analysis of fluid-fluid immiscibility in cholesterol-phospholipid systems.

Incorporation of cholesterol into either egg PC or DMPC membranes immediately inhibited the occurrence of vertical fluctuations. Feix et al. (32) have previously noted that vertical fluctuations are diminished in unsaturated as compared with saturated host lipids (see, for example, the 0 mol% data point in Figs. 8 and 9). For comparison, in membranes composed entirely of 1-palmitoyl-2-oleoylphosphatidylcholine (POPC), which contains a single *cis* double bond in the *sn*-2 alkyl chain, the relative 16:5 exchange rate $W_{Hex}(16:5)/W_{Hex}(16:16)$ is decreased by 28% relative to DMPC at 37°C (32). Incorporation of 30 mol% cholesterol diminishes the relative 16:5 exchange rate by 48% in egg PC and by 63% in DMPC (Fig. 9). Thus cholesterol produces a far greater inhibition of vertical fluctuations than does the presence of a single *cis* double bond.

The effects of cholesterol on spin-label motion were greater in DMPC than in egg PC as indicated by ELDOR measurements of lateral diffusion (Fig. 7) and vertical fluctuations (Figs. 8, 9) and CW ESR observation of the order parameter (Fig. 10). These results are consistent with previous studies that indicate that in fluid phase bilayers the effects of cholesterol on the rotational mobility of spin probes (6, 33) and the lateral diffusion of fluorescent lipid analogues (6) become less pronounced when the host lipids have unsaturated rather than fully saturated alkyl chains.

This work was supported by grants GM 27665, GM 22923, and RR 01008 from the National Institutes of Health. J.-J. Yin was also supported by the Biophysics Program at the Medical College of Wisconsin.

Received for publication 29 December 1986 and in final form 3 August 1987.

REFERENCES

1. Quinn, P. J. 1981. The fluidity of cell membranes and its regulation. *Prog. Biophys. Mol. Biol.* 38:1–104.
2. Hemminga, M. A. 1975. An ESR study of the mobility of the cholestane spin label in oriented lecithin-cholesterol multibilayers. *Chem. Phys. Lipids.* 14:141–173.
3. Schreier-Muccillo, S., K. W. Butler, and I. C. P. Smith. 1973. A spin probe study of the influence of cholesterol on motion and orientation of phospholipids in oriented multibilayers and vesicles. *Chem. Phys. Lipids.* 10:11–27.
4. Dahl, C. E. 1981. Effect of sterol structural on acyl chain ordering in phosphatidylcholine vesicles: a deuterium nuclear magnetic resonance and electron spin resonance study. *Biochemistry.* 20:7158–7161.
5. Taylor, M. G., and I. C. P. Smith. 1980. The fidelity of response by nitroxide spin probes to changes in membrane organization. *Biochim. Biophys. Acta.* 599:140–149.
6. Kusumi, A. K., A. K. Subczynski, M. Pasenkiewicz-Gierula, J. S. Hyde and H. Merkel. 1986. Spin-label studies on phosphatidylcholine-cholesterol membrane: effect of acyl chain length and unsaturation in fluid phase. *Biochim. Biophys. Acta.* 854:307–317.
7. Presti, F. T., R. J. Pace, and S. I. Chan. 1982. Cholesterol-phospholipid interaction in membrane. II. Stoichiometry and molecular packing of cholesterol-rich domains. *Biochemistry.* 21:3831–3835.
8. Lentz, B. R., D. A. Barrow, and M. Hoechli. 1980. Cholesterol-phosphatidylcholine interaction in multilamellar vesicles. *Biochemistry.* 19:1943–1954.
9. Kutchai, H., L. H. Chankler, and G. B. Zavoico. 1983. Effect of cholesterol on acyl chain dynamics in multilamellar vesicles of various phosphatidylcholines. *Biochim. Biophys. Acta.* 736:137–149.
10. Rubenstein, J. L. R., B. A. Smith, and H. M. McConnell. 1979. Lateral diffusion in binary mixtures of cholesterol and phosphatidylcholine. *Proc. Natl. Acad. Sci. USA.* 76:15–18.
11. Alecio, M. R. D. E. Golan, W. A. Veatch, and R. R. Rando. 1982. Use of a fluorescent cholesterol derivative to measure lateral mobility of cholesterol in membranes. *Proc. Natl. Acad. Sci. USA.* 79:5171–5175.
12. Wu, E.-S., K. Jacobson, and D. Papahadjopoulos. 1977. Lateral diffusion in phospholipid multibilayers measured by fluorescence recovery after photobleaching. *Biochemistry.* 16:3936–3941.
13. Kuo, A.-L., and C. G. Wade. 1979. Lipid lateral diffusion by pulse nuclear magnetic resonance. *Biochemistry.* 18:2300–2308.
14. Lindblom, G. L., L. B.-A. Johansson, and G. Arvidson. 1981. Effect of cholesterol in membranes. Pulse nuclear magnetic resonance measurements of lipid lateral diffusion. *Biochemistry.* 20:2204–2207.

15. Popp, C. A., and J. S. Hyde. 1982. Electron-electron double resonance and saturation recovery studies of nitroxide electron and nuclear spin-lattice relaxation times and Heisenberg exchange rates: lateral diffusion in dimyristoyl phosphatidylcholine. *Proc. Natl. Acad. Sci. USA.* 79:2259–2563.
16. Feix, J. B., C. A. Popp, S. D. Venkataramu, A. H. Beth, J. H. Park, and J. S. Hyde. 1984. An electron-electron double resonance study on interaction between [^{14}N] and [^{15}N] stearic acid and vertical fluctuation in dimyristoylphosphatidylcholine. *Biochemistry.* 23:2293–2299.
17. Hyde, J. S., J.-J. Yin, W. Froncisz, and J. B. Feix. 1985. Electron-electron double resonance (ELDOR) with a loop-gap resonator. *J. Magn. Reson.* 63:142–150.
18. Lai, C.-S., M. D. Wirt, J.-J. Yin, W. Froncisz, J. B. Feix, T. J. Kunicki, and J. S. Hyde. 1986. Lateral diffusion of lipid probes in the surface membrane of human platelets. An electron-electron double resonance study. *Biophys. J.* 50:503–506.
19. Devaux, P., and H. M. McConnell. 1972. Lateral diffusion in spin labeled phosphatidylcholine multilayers. *J. Am. Chem. Soc.* 94:4475–4481.
20. Recktenwald, D. J., and H. M. McConnell. 1981. Phase equilibria in binary mixtures of phosphatidylcholine and cholesterol. *Biochemistry.* 20:4505–4510.
21. Kevan, L., and L. D. Kispert. 1976. Electron Spin Double Resonance Spectroscopy. John Wiley & Sons, Inc., New York. 427 pp.
22. Hyde, J. S., J. C. W. Chien, and J. H. Freed. 1968. Electron-electron double resonance of free radical in solution. *J. Chem. Phys.* 48:4211–4226.
23. Venkataramu, S. D., D. E. Pearson, A. H. Beth, K. Balasubramanian, C. R. Park, and J. H. Park. 1983. Synthesis of ^{15}N-5-doxylstearic acid for improved EPR characterization of lipid motion in biomembranes. *J. Labeled Comp. D. & Radiopharm.* 20:433–445.
24. Popp, C. A., and J. S. Hyde. 1981. Effects of oxygen on ESR spectra of nitroxide spin-label probes of model membranes. *J. Magn. Reson.* 43:249–258.
25. Eastman, M. P., G. V. Bruno, and J. H. Freed. 1970. ESR studies of Heisenberg spin exchange. III. An ELDOR study. *J. Chem. Phys.* 52:321–327.
26. Huisjen, M., and J. S. Hyde. 1974. A pulsed EPR spectrometer. *Rev. Sci. Instrum.* 45:669–675.
27. Yin, J.-J., M. Pasenkiewicz-Gierula, and J. S. Hyde. 1987. Lateral diffusion of lipids in membrane by pulse saturation recovery electron spin resonance. *Proc. Natl. Acad. Sci. USA.* 84:964–968.
28. Hubbell, W. L., and H. M. McConnell. 1971. Molecular motions in spin-labeled phospholipids and membranes, *J. Am. Chem. Soc.* 93:314–326.
29. Stanley, K. J., and R. A. Vaughn. 1969. Electron Spin Relaxation Phenomena in Solids. Plenum Publishing Corp., New York. 1–62.
30. Yoshida, H., D.-F. Feng., and L. Kevan. 1973. Electron-electron double resonance study of trapped electrons in γ-irradiated 2-methyltetrahydrofuran glass: magnetic energy transfer between two different spin systems. *J. Chem. Phys.* 58:4924–4929.
31. Freed, J. H. 1979. Theory of multiple resonance and ESR saturation in liquids and related media. *In* Multiple Electron Resonance Spectroscopy. M. M. Dorio and J. H. Freed, editors. Plenum Publishing Corp., New York. 73–142.
32. Feix, J. B., J.-J. Yin, and J. S. Hyde. 1987. Interaction of ^{14}N:^{15}N stearic acid spin-label pairs: effects of host lipids alkyl chain length and unsaturation. *Biochemistry.* 26:3850–3855.
33. Guyer, W., and K. Bloch. 1983. Phosphatidylcholine and cholesterol interactions in model membranes. *Chem. Phys. Lipids.* 33:313–322.